Edinburgh Research Explorer

Longitudinal transcriptome analysis of cattle infected with Theileria parva

OPEN ACCESS

1   **Longitudinal transcriptome analysis of cattle infected with *Theileria***

2   ***parva***

3   Chepkwony, M.[1][§], Wragg, D.[2][§], Latré de Laté, P.[1], Paxton, E.[2], Cook, E.[1], Ndambuki, G.[1], Kitala,

4   P.[3], Gathura, P.[3], Toye, P.[1][†][*], Prendergast, J.[2][†][*]

5

6   [1] Centre for Tropical Livestock Genetics and Health (CTLGH), ILRI Kenya, P.O. Box 30709,

7   Nairobi 00100, Kenya

8   [2] Centre for Tropical Livestock Genetics and Health (CTLGH), Easter Bush Campus, EH25

9   9RG, UK

10   [3] College of Agriculture and Veterinary (CAVS), University of Nairobi, P.O. Box 29053-00624,

11   Kangemi, Nairobi, Kenya.

12

13   [§] Maurine Chepkwony and David Wragg contributed equally to this work

14   [†] Philip Toye and James Prendergast contributed equally to this work

15   [*] Corresponding authors, James Prendergast: james.prendergast@roslin.ed.ac.uk and Philip

16   Toye:p.toye@cgiar.org

17

18

Note: Supplementary data associated with this article

Abstract

The apicomplexan cattle parasite *Theileria parva* is a major barrier to improving the livelihoods of smallholder farmers in Africa, killing over one million cattle on the continent each year. Although exotic breeds not native to Africa are highly susceptible to the disease, previous studies have illustrated that such breeds often show innate tolerance to infection by the parasite. The mechanisms underlying this tolerance remain largely unclear. To better understand host response to *T. parva* infection we characterised the transcriptional response over 15 days of tolerant and susceptible cattle (n=29) naturally exposed to the parasite. We identify key genes and pathways activated in response to infection as well as, importantly, several genes differentially expressed between the animals that ultimately survived or succumbed to infection. These include genes linked to key cell proliferation and infection pathways. Furthermore, we identify response expression quantitative trait loci containing genetic variants whose impact on the expression level of nearby genes changes in response to the infection. These therefore provide an indication of the genetic basis of differential host response. Together these results provide a comprehensive analysis of the host transcriptional response to this under-studied pathogen, providing clues as to the mechanisms underlying natural tolerance to the disease.

Key words

RNA, gene expression, host, parasite, Boran, tolerance, theileria.

2

1. Introduction

The apicomplexan parasite *Theileria parva* infects cattle and buffalo causing a fatal lymphoproliferative disease in the former known as either East Coast Fever (ECF) or Corridor disease. ECF is transmitted from cattle to cattle by the tick *Rhipicephalus appendiculatus*, while Corridor disease occurs when the parasite is transmitted from buffalo to cattle by the same vector (Nene and Morrison, 2016; Cook et al., 2021). In susceptible animals, fatality rates from the diseases are over 90%, causing an estimated economic impact of over US$300 million annually to African farmers (Mukhebi and Perry, 1992; Tretina et al., 2015). However, previous work has illustrated that several native African breeds show elevated survival following exposure to the disease, suggestive of genetic tolerance. For instance, Ndungu *et al.* (2005) reported differential susceptibility of different cattle breeds in Kenya to the infection, with exotic and improved cattle breeds being more susceptible than indigenous cattle breeds. More recently, tolerance has been observed within a line of Boran cattle exposed to *T. parva* (Sitt et al., 2015; Latre de Late et al., 2021) and a genomic region of about 6 Mbp has been shown to be highly associated with the tolerance phenotype in these cattle (Wragg et al., 2022).

Previous studies of ECF have described the pathogenesis in detail (Lawrence et al., 2004), in addition to changes in parasite gene expression during infection (Bishop et al., 2005; Tonui et al., 2018; Atchou et al., 2020). As with other apicomplexan parasites, the Theileria species are known to hijack host gene expression during infection. By co-opting host cellular pathways of infected T and B cells, the parasites can transform the host cells and induce uncontrolled proliferation. Key host targets include repression of the NF-κB apoptotic pathway and elevated expression of metalloproteases that have been linked to invasion. Studies on the involvement of host genes during infection have largely focused on specific candidate genes within these pathways (Eichhorn et al., 1990; Heussler et al., 2001; Dessauge et al., 2005a; Tretina et al., 2020) and little is known of the genome-wide host transcriptional response during *T. parva*

3

66   infection. Further understanding host transcriptional changes is likely to provide important

67   insights into the effects of infection and how the host responds.

68   Understanding of *T. parva* pathogenetic processes has benefitted considerably from studies on

69   the related parasite *Theileria annulata* which also infects cattle and immortalizes infected cells.

70   *T. annulata* infects and transforms B cells and monocytes whereas *T. parva* transforms T cells

71   and B cells, with infected T cells being considered the more pathogenic (Emery et al., 1988;

72   Spooner et al., 1989; Morrison et al., 1996; Tindih et al., 2012). As a result, the pathways

73   involved in host cell infection and transformation may differ due to the cell types involved. An

74   example is the interferon production by infected cells. Interferon gamma production has been

75   associated with *T. parva*-infected T cells only, while *T. annulata*-infected cells has been

76   associated with interferon beta production (Ahmed et al., 1993; Sager et al., 1998).

77   As well as informing its role in cattle disease, the study of *T. parva* infection also has relevance

78   to human diseases. *T. parva* is related structurally and functionally to other apicomplexan

79   parasites, including the Plasmodium species that cause malaria. *T. parva* infects lymphocytes,

80   immortalizing them into exponentially dividing lymphoblasts with metastatic capacity similar to

81   that of cancerous cells (Fry et al., 2016; Tretina et al., 2020). *T. parva* transformed cells share a

82   range of hallmarks with cancer cells which influence the pathogenesis of the infection including,

83   for example, impairment of the apoptotic process contributing to the immortalization of infected

84   cells (Heussler et al., 1999). Similarly, the exponential proliferation of infected cells is another

85   hallmark shared between *T. parva*-infected cells and cancer cells. This has been associated

86   with production of certain cytokines that mediate this process in addition to changes in the

87   transcription factors involved in regulation of the cell cycle (Eichhorn et al., 1990; Dobbelaere et

88   al., 2000; Heussler et al., 2001; Tretina et al., 2020). It has been proposed that a better

89   understanding of host-Theileria interactions may identify cancer drugs that can be co opted to

4

90 treat Theileria infection, as well as, potentially, provide insights into the shared mechanisms

91 underlying cellular immortalization (Tretina et al., 2015).

92 Here, we characterise the transcriptional response in cattle across the course of natural

93 infection with buffalo derived *T. parva*. This study investigates changes in the expression of host

94 genes during infection and associated biological pathways. In addition, we compare gene

95 expression profiles between animals that survived infection to those that succumbed, providing

96 insights into potential mechanisms underlying tolerance to infection.

97 **2. Materials and Methods**

98 The study protocols were approved by the International Livestock Research Institute's (ILRI's)

99 Institutional Animal Care and Use Committee (Reference 2018-10).

100 **2.1. Field challenge and sampling**

101 In 2018, 30 Boran cattle from the Kapiti research station in Machakos county, a region of low *T.*

102 *parva* prevalence, were transported to the Ol Pejeta Conservancy (Nanyuki, Kenya) where they

103 were naturally exposed to buffalo-derived *T. parva*. The cattle were part of an ongoing study

104 investigating genetic tolerance to East Coast fever, and their pedigree was known. Cattle were

105 tested by enzyme linked immunosorbent assay (ELISA) using an established protocol to ensure

106 no prior exposure to *T. mutans* and *T. parva* infection (Katende et al., 1998). While at Ol Pejeta,

107 cattle were kept in an area of the ranch free from other cattle, but in the presence of buffalo.

108 Whole blood samples were collected in 10 ml EDTA (ethylenediaminetetraacetic acid) tubes

109 prior to transporting cattle to Ol Pejeta (day 0) and exposure to *T. parva*, to characterise innate

110 differences between the cattle. Additional blood sampling was conducted on days 7 and 15 of

111 the trial to compare differences in transcriptome profiles during infection. Infection with *T. parva*

112 was confirmed by microscopy of lymph node smears.

2.2. Isolation of white blood cells (WBCs) and RNA

Blood (4-5 ml) was transferred into 15ml falcon tubes containing 10 ml red blood cell lysis buffer (tris NH4CL2) and incubated at room temperature (RT) for 5 minutes. Tubes were then centrifuged at 300 xg for 5 mins at RT and the supernatant discarded. The pellet was rinsed twice with 15 ml of phosphate buffered saline (PBS) and centrifuged at 300 xg for 5 mins each time. The pellet was resuspended in 1.4 ml of tri-reagent, mixed using a pipette to form a homogenous lysate, and a 0.7 ml aliquot incubated at RT for 5 mins before storing at –20°C. At the end of the field trial, samples were transferred to ILRI Nairobi and stored at –80°C until RNA extraction.

RNA was extracted by phenol chloroform extraction as follows. The WBCs in tri-reagent were thawed at RT, vortexed briefly to homogenize the lysate, 0.2 ml of chloroform added and left to incubate at RT for 3 mins before being centrifuged for 15 mins at 12000 xg at 4°C. The aqueous phase containing the RNA was collected by pipette and transferred into a sterile microtube, to which 1.5 ml of isopropanol was added and left to incubate at RT for 10 mins. The sample was then centrifuged for 10 mins at 12,000 xg at 4ºC and the supernatant discarded. The pellet was resuspended in 1 ml of 75% ethanol, vortexed briefly, centrifuged for 5 mins at 7500 xg at 4ºC, supernatant discarded, and pellet left to dry for 10 mins before resuspending in RNAse-free water. RNA quality was assessed by NanoDrop™ spectrophotometer to ensure an A230/280 ratio > 1.8, and by running the sample on a 1.5% agarose gel to check for the presence of 28S, 18S, mRNA and micro-RNA bands. Samples were shipped on dry ice to the Roslin Institute in the UK.

2.3. Processing of RNA-seq data

Library preparation (TruSeq Stranded mRNA) and sequencing of RNA samples was performed by Edinburgh Genomics on the Illumina HiSeq platform. Each sample was sequenced across

137   three lanes with a target coverage of 70 M x 50 bp reads per sample. Sample sequencing

138   qualities were assessed using fastQC (v0.11.7) (Andrews, 2010). Reads were aligned to the

139   *Bos taurus* ARS-UCD1.2 genome assembly (http://ftp.ensembl.org/pub/release-

140   97/fasta/bos_taurus/dna/Bos_taurus.ARS-UCD1.2.dna.toplevel.fa.gz) (Cunningham et al.,

141   2019) using STAR (v2.7.1a; --sjdbOverHang 49 --genomeSAindexNbases 14) (Dobin et al.,

142   2013), for which the ARS-UCD1.2 gene annotation file (http://ftp.ensembl.org/pub/release-

143   97/gtf/bos_taurus/Bos_taurus.ARS-UCD1.2.97.gtf.gz) was also provided. Unmapped reads

144   were subsequently aligned to the *T. parva* ASM16536v1 genome assembly

145   (https://ftp.ncbi.nlm.nih.gov/genomes/all/GCF/000/165/365/GCF_000165365.1_ASM16536v1/G

146   CF_000165365.1_ASM16536v1_genomic.fna.gz) using STAR (--sjdbOverHang 49 --

147   genomeSAindexNbases 10). The resulting sample alignment qualities were assessed using

148   fastQC. Per base sequence content from the fastQC reports were analysed in R. Gene GC

149   content was retrieved within R (v4.0.2) from Ensembl's BioMart (Ensembl Genes 104;

150   btaurus_gene_ensembl; version ARS-UCD1.2) with the biomartr package (Drost and

151   Paszkowski, 2017). Functional profiling of genes in the upper and lower 5% of the distribution of

152   log normalised gene expression ratios (day 15 / day 0), from equal content-sized bins of day 0

153   gene expression, was performed using the g:GOSt tool of g:Profiler (Raudvere et al., 2019). All

154   expressed genes were provided as the custom domain space, the query list of genes was

155   ordered by log normalised gene expression ratio, and an ordered query performed with the

156   g:SCS algorithm (Reimand et al., 2007).

157   Non-parametric Wilcoxon tests were used in Figures 1 and 2 as the underlying data was

158   generally not normally distributed.

159

2.4. Differential gene expression analyses

Mapped reads were summarised using featureCounts (-F "GTF" -t "exon" -g "gene_id") (Liao et al., 2014). The gene counts were then analysed for differential gene expression using the DESeq2 R package (Love et al., 2014). We ran a likelihood ratio comparison between the full model with an interaction term between day and status (design = ~ day + sex + group + status + day:status) and a reduced model (reduced = ~day + sex + group). Covariate factors were sex (M or F), day (0, 7, or 15), and group (pedigree or unrelated), while status was a binary indicator of survival outcome. We also fit independent models for each day (design = ~ sex + group + status) and compared to a reduced model (reduced = ~ sex + group). Model comparisons were performed using likelihood ratio tests (LRTs).

Log_2 fold change and p value outputs were considered for the description of DEGs. We explored genes that were significantly differentially expressed at a false discovery rate (FDR) of ≤ 0.05 as well as those that were differentially expressed at a nominal p value of < 0.01, or had a log_2 fold change > 1. The gene lists generated from these comparisons were used for gene set enrichment analyses (GSEA). LRT results for these genes were clustered using the hierarchical clustering implementation tool DEGreport (Pantano et al., 2021).

2.5. eQTL and reQTL analyses

Statistical modeling was performed in R (v4.0.2). Expression quantitative trait loci (eQTL) analyses were performed using DESeq2 normalised gene expression values and Illumina BovineHD genotype data generated by Wragg et al. (2022). To identify eQTL within each time point for each gene and *cis* variant we fit a linear model of gene expression against allele dosage at the *cis* variant, accounting for sex (male or female) and group (pedigree or unrelated)

182   as factors. A *cis* variant included any bi-allelic variant within 1 Mb upstream and 1 Mb

183   downstream of the gene's start and end positions, respectively, with a minor allele frequency >

184   0.1. Within each time point we adjusted the eQTL F-statistic p values to FDRs. From the eQTL

185   models we sought to identify response eQTL (reQTL) by performing a beta-comparison of

186   regression slopes. Briefly, regression coefficients (□) and variance (□) were calculated for each

187   eQTL and compared between time points using a z-test:

188
$$z = \frac{\beta_a dayA - \beta_b dayB}{\sqrt{\sigma^2 dayA + \sigma^2 dayB}}$$

189

190   **2.6. Functional enrichment analyses**

191   We employed the Database for Annotation, Visualization, and Integrated Discovery (DAVID),

192   functional annotation tool (Huang et al., 2009) to test for functional enrichment. This was further

193   supplemented by analysis of the same genes using the Functional Mapping and Annotation of

194   Genome-Wide Association Studies (FUMA-GWAS) tool (Watanabe et al., 2017) using the

195   Gene2Func function.

196   **3. Results**

197   Pedigree, gender and survival details for the animals in the study are provided in

198   Supplementary Table S1. One animal was killed by a lion on day nine of the trial and thus was

199   lost to follow up study. We analysed the transcriptional response of the remaining 29 Boran

200   cattle exposed to field infection with *T. parva*. Among them, 23 were progeny of three sibling

201   sires (sire 1 n=5; sire 2 n=9; sire 3 n=9), which we refer to below as "pedigree" animals, while

202   six were unrelated. In total, 20 cattle succumbed to infection (dead, treated or euthanised) while

203   nine cattle survived without intervention. The mean time to death or intervention was 20.4 days.

9

204   Some samples for a given time point did not produce sequence data due to low RIN scores

205   (RNA integrity number), giving a total of 28, 23 and 28 samples at days 0, 7 and 15,

206   respectively.

207   **3.1. Transcriptome base sequence content diverges post-infection**

208   Analysis of *B. taurus*-aligned reads revealed a marked global transcriptional response during

209   the 15 days following translocation to the field site, with a clear shift in the GC content of

210   transcribed genes (Fig 1A). Whereas the median GC content of transcripts expressed at day 0

211   was 50.9 ± 4.24 SD, this increased to 54 ± 4.15, on day 7 and 55 ± 3.99 on day 15 (Wilcoxon p

212   < 0.05, Fig 1B). Breaking down genes by their expression level on day 0 highlighted that highly

213   expressed genes with a low GC content are more likely to decrease in their relative expression

214   levels over the course of the infection (Fig 1C,D). These results indicate a general

215   transcriptional response to infection linked to the GC content of genes.

216   To further illustrate this, we undertook functional analysis of highly expressed genes (Fig 1D)

217   whose log normalised expression ratio (day 15 / day 0) was in the upper or lower 5% of the

218   distribution, and which had a low (≤ 41.7) or high (≥ 51.1) GC content. In particular, we find

219   significant enrichment (g:SCS adjusted $P < 0.05$) of the TSLP and TGF-β signalling pathways

220   among low GC content genes exhibiting a reduction in relative expression, and for a range of

221   immune-related terms among high GC content genes exhibiting an increase in relative

222   expression (Supplementary Tables S2-S5).

223

224

3.2. Analysis of unmapped reads confirms *T. parva* infection

Reads that failed to align to the *B. taurus* genome were aligned to the *T. parva* genome to study parasite expression. We observed a 20-fold increase in the proportion of these reads that aligned to the *T. parva* genome from background levels on day 0, (median 3562 ± 3762 SD reads) to day 15 (median 71511 ± 124551). The relative increases in the proportion of *T. parva*-aligned reads were significant at both day 7 (Wilcoxon p = 0.0084) and day 15 (Wilcoxon p = 1 x 10^{-15}; Fig 2A). Comparing the day 15 proportion of *T. parva*-derived reads between animals that died (n = 15), were treated (n = 2) or euthanised (n = 2) due to severe illness, to those that survived (n = 9) returned a Wilcoxon p value of 0.076, with survivors possessing, on average, the smallest proportion of *T. parva*-derived reads (Fig 2B).

3.3. Host genes change in expression pattern throughout the course of the field trial

A principal component analysis (PCA) of normalised bovine gene expression levels revealed both a clear differentiation of samples collected before and after exposure to *T. parva* along PC1, and divergence between samples collected at days 7 and 15 on PC2 (Fig 3). To identify genes differentially expressed across the course of infection (DEGs) a time course analysis across the three days (0, 7 and 15) was carried out. When accounting for survival status, sex, and relatedness (pedigree or unrelated), DEGs significant at FDR < 0.05 clustered into four groups (Fig 4A) which can broadly be described as: (1) genes whose expression is relatively high on day 7 but reduced by day 15 (cluster 1, n= 2603); (2) genes that have higher expression on day 7 and remain so on day 15 (cluster 2, n= 6095); (3) genes that show a gradual increase in expression from day 0 to 15 (cluster 3, n= 748); and (4) genes whose relative expression is lower at day 15 compared to day 0 (cluster 4, n= 7238).

248   Gene set enrichment analysis (GSEA) was performed to identify gene ontologies and pathways

249   that were enriched across the genes within the different clusters (Table 1). A more detailed

250   presentation of the data can be found in Supplementary Fig S1. Many of the annotations

251   identified are linked to the establishment of infection, cell proliferation, cell death or metastasis.

252   Cytokine signalling through the JAK-STAT pathways among others are highlighted. These

253   include proinflammatory cytokines like interleukin 6 (*IL6*), tumor necrosis factor alpha (*TNFα*)

254   and interferons gamma and alpha (*IFNγ*, *IFNα*), which have all been described to increase in

255   production in Theileria infections (McGuire et al., 2004; Razmi et al., 2019), where they

256   potentially contribute towards survival, invasiveness, and metastasis of Theileria transformed

257   cells (Ma and Baumgartner, 2014). Some genes which are targets of either *E2F* or *MYC* are

258   enriched among cluster 2 genes. *E2F* and *MYC* related pathways have been shown to play a

259   role in enhancing survival and proliferation of Theileria-infected cells (Dessauge et al., 2005a;

260   Tretina et al., 2020). The JAK/STAT3 signalling pathway has previously been suggested to

261   contribute to *c-Myc* activation and is associated with host cell transformation by Theileria

262   (Dessauge et al., 2005a), which is supported by our results showing that genes involved in the

263   IL6_JAK_STAT3 signalling pathway are differentially expressed on days 7 and 15. Other

264   pathways highlighted include the tumour protein 53 (*P53*) and members of class O of forkhead

265   box transcription factor (*FoxO*) signalling pathways - which have been associated with apoptosis

266   of host proliferating cells (Haller et al., 2010; Aster et al., 2017). *P53* is a pro-apoptotic protein

267   whose expression is directly dependent on parasite interaction (Haller et al., 2010). In our study,

268   *P53* shows higher expression (Fig 4B) on days 7 and 15 compared to day 0. *P53* interacts with

269   *TNFα*-activated nuclear factor kappa beta (*NFkB*) competitively and they inhibit each other's

270   activities (Webster and Perkins, 1999; Dobbelaere et al., 2000). *TNFα* signalling via *NFkB*,

271   which is enriched among cluster 3 genes, is not only involved in pro-apoptotic and pro-survival

272   signals but also promotes invasiveness and metastasis of Theileria-transformed cells (Ma and

273 Baumgartner, 2014). In this study, expression of NFkB was highest prior to infection by *T.*

274 *parva*, and the number of transcripts reduced along the course of infection (Fig 4B). This is

275 contrary to previous results which described NFkB to be persistently induced by *T. parva*

276 infection and is required for T cell activation and proliferation (Palmer et al., 1997). Genes

277 involved in IL2-STAT5 signalling are differentially expressed among cluster 1 genes. *IL2* is a

278 primary growth factor for activated T cells in this pathway (Mahmud et al., 2013). We observe a

279 marginal but non-significant increase in *IL2* expression at day 7, and a significant (Wilxocon p <

280 0.05) decrease by day 15, while *IL2* receptors (*IL2RA*, *IL2RB* and *IL2RG*) show a significant

281 increase in expression at day 15 (Fig 4C).

282

283 Table 1: Biological functions/pathways significantly enriched (FDR ≤ 0.05) in gene clusters

284 showing differential expression across time in *T. parva* infected cattle.

Annotation	Pathways enriched in gene clusters (from Fig 4A)			
	1	2	3	4
Complement	●			
Epithelial-mesenchymal transition	●			
Apical junction	●			
KRAS signalling	●			
IL2_STAT5 signalling	●		●	
Hypoxia	●			●
Oxidative phosphorylation		●		
MYC targets		●		
DNA replication		●		
Biosynthesis of amino acids		●		
Fatty acid metabolism		●		
Mitochondrial translation		●		
E2F		●		
Mitochondrion		●	●	
Nucleoplasm				●
Interferon gamma response		●	●	
Apoptotic process		●		
Ribonucleotide binding		●		●

T cytotoxic pathway		●		
MAPK pathway		●		
EDG1 pathway		●		
AHSP pathway		●		
TCR pathway		●		
Inflammatory response			●	
Cell response to lipopolysaccharide			●	
Allograft rejection			●	
Chemokine signalling pathway			●	
Interferon Alpha response			●	
IL6_JAK_STAT3 signalling			●	
TNFA signalling via NFKB			●	●
TGF beta signalling			●	
TH1TH2 pathway			●	
TID pathway			●	
Reck pathway			●	
Apoptosis				●
P53 pathway				●
Regulation of cell proliferation			●	
Defense response			●	

285   Enrichment analyses were conducted with FUMA and DAVID, and reported only where both

286   tools returned FDR <0.05 in the categories: hallmark gene sets, KEGG pathways, Biocarta

287   pathways, GO biological processes, GO cellular components, and GO molecular functions.

288   Detailed results are presented in Supplementary Fig S1.

289

3.4. Expression pattern of certain genes is different in surviving and susceptible cattle

291   To investigate whether there was potentially a different transcriptional response in the animals

292   that survived infection, we compared those that died, were euthanised or were treated to those

293   that survived and had cleared the parasite from their lymph node smears by the end of the trial

294   without intervention (Fig 2B: survived group). We identified 64 genes significantly differentially

295   expressed between the dead and survivor cattle across the timepoints at a FDR < 0.05. The

296   majority of genes clustered into 2 groups reflecting a reduction (cluster 1 n=22) or an increase

297   (cluster 2 n=34) in expression levels following field exposure to infection.

298   The most significant differentially expressed gene (FDR = 5.0 x 10^{-4}) was kinesin family member

299   12 (*KIF12*), which was expressed more highly in the survivor group on day 15. *KIF12* has been

300   reported to play a critical role in cell division, specifically in cytokinesis (Lakshmikanth et al.,

301   2004), and in cellular response to oxidative stress (Yang et al., 2014). Other highly differentially

302   expressed genes with known functions include RNA binding motif protein 3 (*RBM3*) for which

303   high expression has been associated with increased survival rates for patients with certain types

304   of cancers (Pilotte et al., 2018; Gao et al., 2020). Although in our analysis, expression of *RBM3*

305   generally decreased following infection, its expression was higher in cattle that survived.

306   Vasohibin1 (*VASH1*) inhibits proliferation and migration of endothelial cells thus limiting the

307   metastasis of tumor cells in cancers (Du et al., 2017; Zhao et al., 2017; Wang et al., 2019) as

308   well as protecting endothelial cells from the effects of toxic stress (Miyashita et al., 2012).

309   *VASH1* expression generally increased following infection and was significantly higher (FDR =

310   0.0012) in cattle that survived infection. High mobility group box 3 (*HMGB3*), which has been

311   shown to have pro-proliferative and pro-metastatic effects in cancer cells (Nemeth et al.,2005,

312   2006; Guo et al., 2016; Liu et al., 2018), decreased in expression from day 0 to day 15 and was

313   more highly expressed in survivor cattle. Interferon induced protein with tetratricopeptide

314   repeats 1 (*IFIT1*) was the most upregulated gene in survivors among the significant DEGs

315   (log2fold change = 3.73), followed by protein C receptor (*PROCR*) (Supplementary Table S6).

316   *IFIT1* has roles in immune response, metastasis, and apoptosis and has been described to

317   have increased expression in cancers (Critchley-Thorne et al., 2007; McDermott et al., 2012;

318   Wah et al., 2018; Pidugu et al., 2019) while certain alleles of the gene have been linked to better

319   malaria prognosis (Wah et al., 2018). In our study, *IFIT* expression generally reduced across

320   time but was higher in the survivors than those that subsequently died. Syntaxin-binding protein

321   1 (*STXBP1*) was the most down regulated gene among the significant DEGs (Log$_2$ fold change

322   = -2.73) followed by purinergic receptor P2X3 (*P2RX3*; log$_2$ fold change = -2.04), both of which

323   follow the cluster 2 expression pattern across time. We performed GSEA on all 64 significant

324   DEGs (Supplementary Table S6). Toll like receptors (*TLRs*), protein kinase B (*AKT*) and

325   mechanistic target of rapamycin kinase (*MTOR*) immunologic functions and pathways were

326   found to be enriched, and are widely reported to play a role in *T. parva* infection in the literature

327   (Heussler et al., 2001; Chi, 2012; Kinnaird et al., 2013; Kamau et al., 2016; Saxton and Sabatini,

328   2017; Kim and Guan, 2019). *AKT* and *MTOR* enrichment was associated with 4 genes (*IFIT1*,

329   *KCNE3*, *KLRB1* and *DLG4*), and although *AKT* and *MTOR* can interact affecting cell survival

330   (Hay and Sonenberg, 2004), they are not reported to interact directly with one another (based

331   on a STRING db analysis; (Szklarczyk et al., 2019)).

332   We next assessed genes that were differentially expressed between survivors and those that

333   subsequently died at specific timepoints, rather than across the time-series as a whole. We ran

334   a similar model using LRTs to identify differentially expressed genes associated with survival

335   status at individual timepoints (days 0, 7 or 15) while accounting for sex and relatedness

336   (pedigree or unrelated). No significant DEGs were found between these groups on day 0 at an

337   adjusted p value of 0.05 (FDR). However, 141 genes were differentially expressed at a nominal

338   p value of 0.01. We considered these as candidate genes that were innately differentially

339   expressed (pre-infection with *T. parva*) between survivors and those that went on to succumb to

340   infection. On day 7, 95 genes that were differentially expressed at a nominal p value of 0.01

341   were considered as genes that responded early to infection, none of which were significant after

342   correcting for multiple testing. At day 15, we identified 11 DEGs (Table 2) with FDR < 0.05 and

343   596 genes with a nominal P < 0.01. Of the 11 DEGs with FDR < 0.05, six (*IGHE*, *TMEM213*,

344   *PKD2L1*, *KIF12*, *IL9R* and *ENSBTAG00000053829*; Fig 5A-F) were also present among the

345   overall significant DEGs in Supplementary Table S6.

346   Among the 11 genes displaying a difference between the animals that survived and succumbed

347   at day 15 the most differentially expressed gene, ENSBTAG00000047632, is a novel gene

348 orthologous (40.94%) to human immunoglobulin heavy constant epsilon (*IGHE*). Human IgE,

349 the product of *IGHE*, has been observed to be upregulated in response to malaria (Duarte et al.,

350 2007). These data suggest this gene shows a differential response in survivors and those that

351 succumbed to *T. parva* infection. ENSBTAG00000048135 (Table 2), another novel gene, is

352 orthologous to several human immunoglobulin heavy constant gamma genes (*IGH1*, 63.50%;

353 *IGHG2*, 65.03%; *IGH3*, 62.58%; *IGH4*, 63.80%). *IGHG2* is the heavy chain of IgG2

354 immunoglobulin whose expression has been associated with protecting individuals against

355 infection with both malaria (Aucan et al., 2000) and *T. parva* (Musoke et al., 1982).

356 Transmembrane protein 213 (*TMEM213*) has been associated with invasion and metastasis in

357 cancers when down regulated and is considered an independent predictor of overall survival in

358 lung cancer with individuals who survive longer showing higher expression of the gene (Zou et

359 al., 2019). In our study, levels of *TMEM213* increased in all cattle across time with survivors

360 having a significantly higher abundance of the gene transcripts. Another notable gene identified

361 is the receptor for interleukin 9 (*IL9R*). *IL9* can play both a tumorigenic role and antitumor role in

362 cancers depending on the interacting molecules (Wan et al., 2020). We observe *IL9* expression

363 to generally reduce in all animals during the field challenge, with abundances being lower in the

364 survivors - although this difference was not significant (p value 0.7, Fig 5G).

365

366 Table 2: Significantly differentially expressed genes (FDR < 0.05) on day 15 between surviving

367 animals and those that succumbed to infection. Gene names in brackets are the human

368 orthologs of cattle genes which remain to be annotated in the cow genome.

Gene stable ID	Gene name	Succumbed/Survivors expression (fold change)	Adjusted P value
ENSBTAG00000047632	(IGHE)	0.16	4.54E-05
ENSBTAG00000049598	H2BC7	0.29	0.011
ENSBTAG00000054686	CRACDL	0.40	0.043
ENSBTAG00000001527	TMEM213	0.14	0.049

ENSBTAG00000048135	(IGHG2)	0.19	0.049
ENSBTAG00000004739	SLC18A2	0.23	0.049
ENSBTAG00000010742	PKD2L1	0.25	0.049
ENSBTAG00000015685	KIF12	0.26	0.049
ENSBTAG00000048257	(CYP4F22)	0.33	0.049
ENSBTAG00000007558	IL9R	0.42	0.049
ENSBTAG00000053829		0.49	0.049

369

370

3.5. Functional enrichment of genes differentially expressed in *T. parva* tolerant cattle

372   DEGs with nominal $p \leq 0.01$ at each day (0,7,15) were separated into lists where their

373   expression was either (i) higher or (ii) lower in cattle that survived infection. Functional

374   enrichment analyses were subsequently performed on each list independently, and the

375   complete results are provided in Supplementary Table S7. Biological pathways and annotations

376   exhibiting significant enrichment ($padj \leq 0.05$) in surviving animals are presented in Fig 6 for

377   each time point. The interferon gamma response was significantly enriched at all three

378   timepoints with different gene sets being associated with the signal at each point

379   (Supplementary Table S7). This suggests that the signalling pathway may be regulated

380   differently between survivors and cattle that succumbed to infection, and that its effect at the

381   various time points may vary depending on the receptors and molecules modulating it. Further

382   investigation of gene interaction networks may help to elucidate the impact of infection by *T.*

383   *parva* on interferon gamma response.

384 At day 0, the nominally significant (p ≤ 0.01) gene set returned enrichment signals across genes

385 that were more highly expressed in survivor cattle compared to those that succumbed to

386 infection, but not for genes with lower expression levels in survivors. Several of the enriched

387 signals returned were previously identified (table 1), including IL2-STAT5 signalling, interferon

388 alpha and gamma response, interleukin-1β secretion, and positive regulation of the *NLRP3*

389 inflammasome complex (Fig 6). *IFIT3* was among four genes associated with interferon alpha

390 response and exhibited higher expression levels in survivors at day 0. Its expression profile was

391 reversed by day 7, with average expression levels being higher in cattle that ultimately

392 succumbed to infection, and by day 15 its expression returned to being higher on average in

393 survivors. However, these differences were not significant after FDR adjustment. *IFIT3* can be

394 induced by either interferon alpha or interferon gamma, and it has been suggested that

395 increased expression of *IFIT3* through *IFN* induction contributes to increased cell survival and a

396 reduction in cellular apoptosis (Hsu et al., 2013).

397 At days 7 and 15, we observe various pathways enriched among genes whose expression is

398 reduced at these time points in survivors relative to cattle that succumbed to infection (Fig 6).

399 These results show that some processes necessary for *T. parva* to infect, proliferate, and

400 metastasize are associated with genes that are expressed at significantly lower levels in cattle

401 that survive infection. The most enriched signal at day 15 was hypoxia, for which the functions

402 of the three most significant genes (*SDC3*, *GPC1* and *PRKCA*) appear to be mediated through

403 interaction with hypoxia inducible factor-1α (*HIF-1α*).

404

405

3.6. Expression quantitative trait loci (eQTL)

406

407 To identify potential genetic drivers of expression differences between samples and timepoints

408 we mapped expression quantitative trait loci (eQTL) and response eQTLs in the cohort. Here an

409 eQTL is a genetic variant whose genotypes are correlated to the expression of a nearby gene at

410 a given time point (Nica and Dermitzakis, 2013). To identify eQTLs, at each time point we fit

411 models testing the association of each gene's expression with *cis* variants, while accounting for

412 sex and relatedness (see methods). Any variant within 1 Mb upstream of a gene's start position

413 and 1 Mb downstream of a gene's end position was considered to be a *cis* variant. After

414 correcting for multiple testing, the proportion of genes with an eQTL (FDR < 0.05) was

415 significantly different between days (chi-sq $p = 1.66 \times 10^{-37}$) with the number of genes identified

416 at day 0 (n = 316) being greater than days 7 (n = 86) and 15 (n = 115), which collectively

417 represented a total of 462 unique genes.

418 These data suggest the impact of genetic variants on gene expression may be changing over

419 the course of the infection. To investigate this further we characterised response eQTLs by

420 comparing the coefficients of eQTLs between timepoints (see methods). The proportion of

421 genes with a response eQTL (reQTL; $|Z| > 4$) was significantly different between pairs of days

422 (chi-sq $p = 3.48 \times 10^{-82}$), with the number of genes identified being greatest between days 0 and

423 15 (n = 1626), followed by day 0 versus day 7 (n = 1282), and day 7 versus day 15 (n = 712),

424 representing a total of 1958 unique genes of which 233 were identified in the previous step as

425 having a significant eQTL. An example of an reQTL associated with the *RTN4IP1* gene is

426 presented in Fig 7.

427 From the significant DEG lists relating to survival, 28 genes with a nominal $p < 0.01$ were also

428 found to have one or more significant eQTL, which is significantly more than expected by

429 chance (chi-sq $p = 0.018$ comparing DEGs with significant eQTL to non-DEGs with significant

430   eQTL). These include *PKD2L1* which was the only DEG with FDR < 0.05 to have a significant

431   eQTL (eQTL on day 15 FDR = 0.008). *VASH1* plays a role in cancer cell metastasis (Ito et al.,

432   2013; Mikami et al., 2017) and had a significant reQTL between days 0 and 7 (Z = -6.2), and

433   days 0 and 15 (Z = 6.5).

434   Functional enrichment of the 28 putative DEGs with significant eQTLs revealed enrichment for a

435   single term: NOTCH signalling (cancer gene module of FUMA software). This signalling

436   pathway was associated with 4 genes in our analysis: *PKD2L1*, *CLSTN3*, *MYO1A* and *HS1BP3*,

437   which suggests that the dysregulation of the NOTCH signalling process in the immune response

438   to *T. parva* infection is dependent on host genetics across these genes.

439   **4. Discussion**

440   This study describes differential expression of genes across time after field exposure to buffalo-

441   derived *T. parva* infection. We report here genes that are differentially expressed in the bovine

442   host and the associated functions enriched among the significantly differentially expressed

443   genes. Our aim in taking this approach was to describe how the host responses evolve in

444   response to buffalo-derived *T. parva* infection. Although the presence of co-infections is

445   possible in field studies, we confirmed the presence of *T. parva* infection in all study animals,

446   ascertained *T. parva* as the cause of death of all cattle regarded as susceptible in this study,

447   and confirmed the presence (Latre de Late et al., 2021) and clearance of *T. parva* parasites

448   from the lymph nodes of all cattle that survived infection.

449   We used peripheral white blood cells for this work. Despite the anticipated lower abundance of

450   parasitized and responding cells in this sample type compared to the draining lymph nodes, we

451   were still able to detect significant signals and genes that are differentially enriched at different

452   time points and cattle groups. These genes can be explored further in *in vitro* cellular studies.

453 The proportion of reads unmapped to the bovine genome that aligned to the *T. parva* genome

454 was very low at days 0 and 7 and is likely attributable to background levels of read mismapping.

455 The source of the *T. parva*-aligned transcripts is presumably macroschizont-infected

456 lymphocytes, as the major form found in peripheral blood in most theilerial infections is the

457 piroplasm, which does not occur regularly in cattle infected with buffalo-derived parasites (Neitz,

458 1957).

459 The response of cattle to *T.parva* exposure is expected to represent both features of the

460 parasite, e.g. its potential to transform and proliferate cells, and the host immune response. The

461 *T. parva* parasite load has been associated with the clinical severity and outcome of disease in

462 cattle (Jura and Losos, 1980; Yamada et al., 2009). We have reported previously that the

463 animals which succumbed to *T. parva* infection in these field studies showed a lymph node

464 parasitosis of earlier onset and greater severity (Latre de Late et al., 2021; Wragg et al., 2022).

465 This led to the working hypothesis that the tolerant cattle limit the proliferation of infected cells.

466 Our current results support this idea, in that there are, potentially fewer *T. parva*-aligned

467 transcripts at day 15 in the animals which survived (p = 0.076). Although it cannot be excluded

468 though that these animals were infected with forms of the pathogens that proliferated less

469 readily, the higher proportion of *T. parva* transcripts in the animals which were treated or

470 euthanized supports the field diagnosis that these animals were undergoing severe disease due

471 to *T. parva* infection. As the last sequencing samples were collected on day 15 and the mean

472 time to death or intervention was 20.4 days, it is likely that further increases in the parasite load

473 occurred and that the proportion of *T. parva*-aligned reads observed on day 15 is an

474 underestimate of the maximum level which occurred.

475 The relatively lower number of parasite transcripts derived from the tolerant cattle was not

476 uniform, in that several susceptible cattle had fewer transcripts than some of the tolerant ones

477   (Fig 2A). It should be noted that the number of parasite transcripts may not be absolutely

478   correlated to the number of infected cells. The number of transcripts detected in circulating

479   lymphocytes depends on the number of infected cells which have migrated from the draining

480   lymph node into the circulation, the number of parasite nuclei per cell and the overall

481   transcriptional activity of the parasite. We cannot at this stage also exclude host genetic effects,

482   such as a decreased sensitivity of tolerant animals to the pathogenic effects of the infected cell,

483   to account for this seemingly anomalous observation.

484   Our results showed good mapping of our reads to the host genome. The divergence observed

485   in base sequence GC content throughout the time course indicates the gross host response to

486   infection and is possibly a result of genes with longer transcripts being expressed, as GC

487   content is proportional to gene length, or possibly an increase in expression of broadly

488   expressed genes, such as housekeeping genes, which typically cluster in GC-rich regions

489   (Lercher et al., 2003; Pozzoli et al., 2008). Functional annotation of GC-rich genes exhibiting the

490   largest change in expression following infection revealed enrichment for immune-related

491   ontologies and pathways, while among genes with low GC content the TSLP and TGF-β

492   signalling pathways were enriched. These pathways are notable as Thymic Stromal

493   Lymphopoietin (TSLP) plays a key role in mediating type 2 immunity (Marković and Savvides,

494   2020), while the production of cytokines by Theileria-infected lymphocytes activate c-MYC - for

495   which TGF-β is a target and activates AP-1 - which is characteristic of Theileria-transformed

496   cells (Dessauge et al., 2005b).

497   There was a clear difference in the expression patterns of host genes before the trial (day 0)

498   and after exposure to the infection (days 7 and 15). Examination of the specific gene expression

499   changes reveals clusters of genes that responded in specific patterns i.e., some were more

500   enhanced at day 7 but not at day 15, while others were persistently enhanced from day 7 up to

501   day 15. We identified genes that have been described to play a role in the establishment of *T.*

502   *parva* infected cells, successful cell proliferation, cell death and metastasis of cells, including:

503   *E2F* (Tretina et al., 2020), *c-MYC* (Dessauge et al., 2005a), and *TNFα* (Guergnon et al., 2003).

504   We also observed genes whose expression was relatively enhanced on day 15 compared to

505   days 0 and 7. These genes are associated with the functions of proliferation, cell death,

506   metastasis, and cellular hypoxia. The main pathway highlighted from our analysis is the JAK-

507   STAT signalling pathway whose primary role is in the transference of cell signals from the

508   membrane to the nucleus, and which is essential for the functioning of cytokines and other

509   growth factors.

510   One of the ways that *T. parva* infected cells have been shown to evade programmed cell death

511   is by manipulating NFkB activation. Our observation of decreasing expression of NFkB across

512   time is contrary to previous results which described persistent induction of NFkB to be essential

513   in *T. parva* infection as it is required for T cell activation and proliferation (Ivanov et al., 1989;

514   Heussler et al., 1999). *T. parva* degrades IkB kinases in the host cell leading to continuous

515   translocation of NFkB to the host cell nucleus and thus prolonged cell survival (Palmer et al.,

516   1997). The contrasting results may be due to the sample type under investigation. Most studies

517   that have described elevated levels of NFkB used cells from *in vitro* cultures, in which most if

518   not all cells are infected, whereas only a small percentage of circulating lymphocytes would be

519   expected to be infected. This may confound the detection of NFkB transcripts in the *T. parva*

520   transformed cell fraction.

521   Investigations into which genes and functions are regulated differently during infection in cattle

522   that are tolerant to *T. parva* infection reveals that although this group of cattle does not exhibit a

523   distinct pattern of gene expression, they do exhibit enhanced responses that might limit cell

524   proliferation and metastasis during infection. *KIF12* is the most significantly differentially

525   expressed gene between tolerant and susceptible cattle, suggesting that differences in cell

24

526 division (cytokinesis) and consequently proliferation between the two groups of cattle might

527 contribute to innate tolerance. KIF12 has not previously been identified in relation to *T. parva*

528 pathogenesis, and is thus an avenue for future research. *RBM3* was also identified, and has

529 been reported to play a role in cell proliferation and cell death (Wellmann et al., 2010). Another

530 key cellular process highlighted among genes significantly differentially expressed between

531 tolerant and susceptible cattle is metastasis, for which *VASH1*, *HMGB3*, *IFIT1* and *TMEM213*

532 were among the identified genes which potentially influence this cellular process.

533 A related publication by Latre de Late *et al.* (2021) using the same animals used in this study,

534 quantified the expression of pro-inflammatory cytokines that have been previously described to

535 have increased expression in Theileria transformed cells (McGuire et al., 2004; Yamada et al.,

536 2009). That study describes an increase in the expression of TGFβ, IL1β, IL6 and TNFα in the

537 susceptible cattle, unlike in the tolerant cattle which maintained a relatively stable expression

538 across time (Latre de Late et al., 2021), broadly in agreement with the observations in our study.

539 Linking gene expression levels to the animal's genotypes we identify a large number of

540 regulatory variants whose links to the expression of nearby genes change through the course of

541 infection. These provide potential initial indications of how the host's response to infection can

542 depend on their genome. However, it should be noted cell type composition differences can

543 confound these kinds of analyses, and future studies on isolated cell types may provide clearer

544 insights into the genetics of host response.

545 **Acknowledgements**

560 **Data availability**

561 RNA sequencing data is available to download from the European Nucleotide Archive under

562 project accession PRJEB39210. Illumina BovineHD genotype data is available to download

563 from Edinburgh DataShare, https://doi.org/10.7488/ds/2985.

564 **References**

565 Ahmed, J.S., Wiegers, P., Steuber, S., Schein, E., Williams, R.O., Dobbelaere, D., 1993.
566   Production of interferon byTheileria annulata-andT. parva-infected bovine lymphoid cell
567   lines. Parasitol. Res. 79, 178–182. https://doi.org/10.1007/BF00931888
568 Andrews, S., 2010. FastQC: A Quality Control Tool for High Throughput Sequence Data.
569 Aster, J.C., Pear, W.S., Blacklow, S.C., 2017. The Varied Roles of Notch in Cancer. Annu. Rev.
570   Pathol. 12, 245–275. https://doi.org/10.1146/annurev-pathol-052016-100127
571 Atchou, K., Ongus, J., Machuka, E., Juma, J., Tiambo, C., Djikeng, A., Silva, J.C., Pelle, R.,
572   2020. Comparative Transcriptomics of the Bovine Apicomplexan Parasite Theileria
573   parva Developmental Stages Reveals Massive Gene Expression Variation and Potential
574   Vaccine Antigens. Front. Vet. Sci. 7, 287. https://doi.org/10.3389/fvets.2020.00287
575 Aucan, C., Traoré, Y., Tall, F., Nacro, B., Traoré-Leroux, T., Fumoux, F., Rihet, P., 2000. High
576   Immunoglobulin G2 (IgG2) and Low IgG4 Levels Are Associated with Human Resistance
577   to Plasmodium falciparum Malaria. Infect. Immun. 68, 1252–1258.
578   https://doi.org/10.1128/IAI.68.3.1252-1258.2000
579 Bishop, R., Shah, T., Pelle, R., Hoyle, D., Pearson, T., Haines, L., Brass, A., Hulme, H.,
580   Graham, S.P., Taracha, E.L.N., Kanga, S., Lu, C., Hass, B., Wortman, J., White, O.,

581   Gardner, M.J., Nene, V., de Villiers, E.P., 2005. Analysis of the transcriptome of the
582   protozoan Theileria parva using MPSS reveals that the majority of genes are
583   transcriptionally active in the schizont stage. Nucleic Acids Res. 33, 5503–5511.
584   https://doi.org/10.1093/nar/gki818
585   Chi, H., 2012. Regulation and function of mTOR signalling in T cell fate decisions. Nat. Rev.
586   Immunol. 12, 325–338. https://doi.org/10.1038/nri3198
587   Cook, E.A.J., Sitt, T., Poole, E.J., Ndambuki, G., Mwaura, S., Chepkwony, M.C., Latre de Late,
588   P., Miyunga, A.A., van Aardt, R., Prettejohn, G., Wragg, D., Prendergast, J.G.D.,
589   Morrison, W.I., Toye, P., 2021. Clinical Evaluation of Corridor Disease in Bos indicus
590   (Boran) Cattle Naturally Infected With Buffalo-Derived Theileria parva. Front. Vet. Sci. 8,
591   1072. https://doi.org/10.3389/fvets.2021.731238
592   Critchley-Thorne, R.J., Yan, N., Nacu, S., Weber, J., Holmes, S.P., Lee, P.P., 2007. Down-
593   Regulation of the Interferon Signalling Pathway in T Lymphocytes from Patients with
594   Metastatic Melanoma. PLOS Med. 4, e176.
595   https://doi.org/10.1371/journal.pmed.0040176
596   Dessauge, F., Hilaly, S., Baumgartner, M., Blumen, B., Werling, D., Langsley, G., 2005a. c-Myc
597   activation by Theileria parasites promotes survival of infected B-lymphocytes. Oncogene
598   24, 1075–1083. https://doi.org/10.1038/sj.onc.1208314
599   Dessauge, F., Lizundia, R., Baumgartner, M., Chaussepied, M., Langsley, G., 2005b. Taking
600   the Myc is bad for Theileria. Trends Parasitol. 21, 377–385.
601   https://doi.org/10.1016/j.pt.2005.06.003
602   Dobbelaere, D.A.E., Fernandez, P.C., Heussler, V.T., 2000. Theileria parva: taking control of
603   host cell proliferation and survival mechanisms. Cell. Microbiol. 2, 91–99.
604   https://doi.org/10.1046/j.1462-5822.2000.00045.x
605   Dobin, A., Davis, C.A., Schlesinger, F., Drenkow, J., Zaleski, C., Jha, S., Batut, P., Chaisson,
606   M., Gingeras, T.R., 2013. STAR: ultrafast universal RNA-seq aligner. Bioinformatics 29,
607   15–21. https://doi.org/10.1093/bioinformatics/bts635
608   Drost, H.-G., Paszkowski, J., 2017. Biomartr: genomic data retrieval with R. Bioinformatics 33,
609   1216–1217. https://doi.org/10.1093/bioinformatics/btw821
610   Du, H., Zhao, J., Hai, L., Wu, J., Yi, H., Shi, Y., 2017. The roles of vasohibin and its family
611   members: Beyond angiogenesis modulators. Cancer Biol. Ther. 18, 827–832.
612   https://doi.org/10.1080/15384047.2017.1373217
613   Duarte, J., Deshpande, P., Guiyedi, V., Mécheri, S., Fesel, C., Cazenave, P.-A., Mishra, G.C.,
614   Kombila, M., Pied, S., 2007. Total and functional parasite specific IgE responses in
615   Plasmodium falciparum-infected patients exhibiting different clinical status. Malar. J. 6, 1.
616   https://doi.org/10.1186/1475-2875-6-1
617   Eichhorn, M., Magnuson, N.S., Reeves, R., Williams, R.O., Dobbelaere, D.A., 1990. IL-2 can
618   enhance the cyclosporin A-mediated inhibition of Theileria parva-infected T cell
619   proliferation. J. Immunol. 144, 691–698.
620   Emery, D. l., Machugh, N. d., Morrison, W. i., 1988. Theileria parva (Muguga) infects bovine T-
621   lymphocytes in vivo and induces coexpression of BoT4 and BoT8. Parasite Immunol. 10,
622   379–391. https://doi.org/10.1111/j.1365-3024.1988.tb00228.x
623   Fry, L.M., Schneider, D.A., Frevert, C.W., Nelson, D.D., Morrison, W.I., Knowles, D.P., 2016.
624   East Coast Fever Caused by Theileria parva Is Characterized by Macrophage Activation
625   Associated with Vasculitis and Respiratory Failure. PLOS ONE 11, e0156004.
626   https://doi.org/10.1371/journal.pone.0156004
627   Gao, G., Shi, X., Long, Y., Yao, Z., Shen, J., Shen, L., 2020. The prognostic and
628   clinicopathological significance of RBM3 in the survival of patients with tumor: A Prisma-
629   compliant meta-analysis. Medicine (Baltimore) 99, e20002.
630   https://doi.org/10.1097/MD.0000000000020002

631 Guergnon, J., Chaussepied, M., Sopp, P., Lizundia, R., Moreau, M.-F., Blumen, B., Werling, D.,
632   Howard, C.J., Langsley, G., 2003. A tumour necrosis factor alpha autocrine loop
633   contributes to proliferation and nuclear factor-κB activation of Theileria parva-
634   transformed B cells. Cell. Microbiol. 5, 709–716. https://doi.org/10.1046/j.1462-
635   5822.2003.00314.x
636 Guo, S., Wang, Y., Gao, Y., Zhang, Y., Chen, M., Xu, M., Hu, L., Jing, Y., Jing, F., Li, C., Wang,
637   Q., Zhu, Z., 2016. Knockdown of High Mobility Group-Box 3 (HMGB3) Expression
638   Inhibits Proliferation, Reduces Migration, and Affects Chemosensitivity in Gastric Cancer
639   Cells. Med. Sci. Monit. 22, 3951–3960. https://doi.org/10.12659/MSM.900880
640 Haller, D., Mackiewicz, M., Gerber, S., Beyer, D., Kullmann, B., Schneider, I., Ahmed, J.S.,
641   Seitzer, U., 2010. Cytoplasmic sequestration of p53 promotes survival in leukocytes
642   transformed by Theileria. Oncogene 29, 3079–3086. https://doi.org/10.1038/onc.2010.61
643 Hay, N., Sonenberg, N., 2004. Upstream and downstream of mTOR. Genes Dev. 18, 1926–
644   1945. https://doi.org/10.1101/gad.1212704
645 Heussler, V.T., Küenzi, P., Fraga, F., Schwab, R.A., Hemmings, B.A., Dobbelaere, D.A.E.,
646   2001. The Akt/PKB pathway is constitutively activated in Theileria-transformed
647   leucocytes, but does not directly control constitutive NF-κB activation. Cell. Microbiol. 3,
648   537–550. https://doi.org/10.1046/j.1462-5822.2001.00134.x
649 Heussler, V.T., Machado, J., Fernandez, P.C., Botteron, C., Chen, C.-G., Pearse, M.J.,
650   Dobbelaere, D.A.E., 1999. The intracellular parasite Theileria parva protects infected T
651   cells from apoptosis. Proc. Natl. Acad. Sci. 96, 7312–7317.
652   https://doi.org/10.1073/pnas.96.13.7312
653 Hsu, Y.-L., Shi, S.-F., Wu, W.-L., Ho, L.-J., Lai, J.-H., 2013. Protective Roles of Interferon-
654   Induced Protein with Tetratricopeptide Repeats 3 (IFIT3) in Dengue Virus Infection of
655   Human Lung Epithelial Cells. PLOS ONE 8, e79518.
656   https://doi.org/10.1371/journal.pone.0079518
657 Huang, D.W., Sherman, B.T., Lempicki, R.A., 2009. Systematic and integrative analysis of large
658   gene lists using DAVID bioinformatics resources. Nat. Protoc. 4, 44–57.
659   https://doi.org/10.1038/nprot.2008.211
660 Ito, S., Miyashita, H., Suzuki, Y., Kobayashi, M., Satomi, S., Sato, Y., 2013. Enhanced Cancer
661   Metastasis in Mice Deficient in Vasohibin-1 Gene. PLOS ONE 8, e73931.
662   https://doi.org/10.1371/journal.pone.0073931
663 Ivanov, V., Stein, B., Baumann, I., Dobbelaere, D.A., Herrlich, P., Williams, R.O., 1989. Infection
664   with the intracellular protozoan parasite Theileria parva induces constitutively high levels
665   of NF-kappa B in bovine T lymphocytes. Mol. Cell. Biol. 9, 4677–4686.
666   https://doi.org/10.1128/MCB.9.11.4677
667 Kamau, E., Nyanjom, S.G., Wamalwa, M., Ng'ang'a, J., 2016. Prediction of protein–protein
668   interactions between Theileria parva and Bos taurus based on sequence homology.
669   Biosci. Horiz. Int. J. Stud. Res. 9. https://doi.org/10.1093/biohorizons/hzw006
670 Katende, J., Morzaria, S., Toye, P., Skilton, R., Nene, V., Nkonge, C., Musoke, A., 1998. An
671   enzyme-linked immunosorbent assay for detection of Theileria parva antibodies in cattle
672   using a recombinant polymorphic immunodominant molecule. Parasitol. Res. 84, 408–
673   416. https://doi.org/10.1007/s004360050419
674 Kim, J., Guan, K.-L., 2019. mTOR as a central hub of nutrient signalling and cell growth. Nat.
675   Cell Biol. 21, 63–71. https://doi.org/10.1038/s41556-018-0205-1
676 Kinnaird, J.H., Weir, W., Durrani, Z., Pillai, S.S., Baird, M., Shiels, B.R., 2013. A Bovine
677   Lymphosarcoma Cell Line Infected with Theileria annulata Exhibits an Irreversible
678   Reconfiguration of Host Cell Gene Expression. PLOS ONE 8, e66833.
679   https://doi.org/10.1371/journal.pone.0066833
680 Lakshmikanth, G.S., Warrick, H.M., Spudich, J.A., 2004. A mitotic kinesin-like protein required

681   for normal karyokinesis, myosin localization to the furrow, and cytokinesis in
682   Dictyostelium. Proc. Natl. Acad. Sci. 101, 16519–16524.
683   https://doi.org/10.1073/pnas.0407304101
684 Latre de Late, P., Cook, E.A.J., Wragg, D., Poole, E.J., Ndambuki, G., Miyunga, A.A.,
685   Chepkwony, M.C., Mwaura, S., Ndiwa, N., Prettejohn, G., Sitt, T., Van Aardt, R.,
686   Morrison, W.I., Prendergast, J.G.D., Toye, P., 2021. Inherited Tolerance in Cattle to the
687   Apicomplexan Protozoan Theileria parva is Associated with Decreased Proliferation of
688   Parasite-Infected Lymphocytes. Front. Cell. Infect. Microbiol. 11, 995.
689   https://doi.org/10.3389/fcimb.2021.751671
690 Lawrence, J.A., Perry, B.D., Williamson, S., 2004. East Coast fever, in: Infectious Disease of
691   Livestock. Oxford University Press, Cape Town, pp. 448–467.
692 Lercher, M.J., Urrutia, A.O., Pavlíček, A., Hurst, L.D., 2003. A unification of mosaic structures in
693   the human genome. Hum. Mol. Genet. 12, 2411–2415.
694   https://doi.org/10.1093/hmg/ddg251
695 Liao, Y., Smyth, G.K., Shi, W., 2014. featureCounts: an efficient general purpose program for
696   assigning sequence reads to genomic features. Bioinformatics 30, 923–930.
697   https://doi.org/10.1093/bioinformatics/btt656
698 Liu, J., Wang, L., Li, X., 2018. HMGB3 promotes the proliferation and metastasis of
699   glioblastoma and is negatively regulated by miR-200b-3p and miR-200c-3p. Cell
700   Biochem. Funct. 36, 357–365. https://doi.org/10.1002/cbf.3355
701 Love, M.I., Huber, W., Anders, S., 2014. Moderated estimation of fold change and dispersion for
702   RNA-seq data with DESeq2. Genome Biol. 15, 550. https://doi.org/10.1186/s13059-014-
703   0550-8
704 Ma, M., Baumgartner, M., 2014. Intracellular Theileria annulata Promote Invasive Cell Motility
705   through Kinase Regulation of the Host Actin Cytoskeleton. PLOS Pathog. 10, e1004003.
706   https://doi.org/10.1371/journal.ppat.1004003
707 Mahmud, S.A., Manlove, L.S., Farrar, M.A., 2013. Interleukin-2 and STAT5 in regulatory T cell
708   development and function. JAK-STAT 2, e23154. https://doi.org/10.4161/jkst.23154
709 Marković, I., Savvides, S.N., 2020. Modulation of Signalling Mediated by TSLP and IL-7 in
710   Inflammation, Autoimmune Diseases, and Cancer. Front. Immunol. 11.
711 McDermott, J.E., Vartanian, K.B., Mitchell, H., Stevens, S.L., Sanfilippo, A., Stenzel-Poore,
712   M.P., 2012. Identification and Validation of Ifit1 as an Important Innate Immune
713   Bottleneck. PLOS ONE 7, e36465. https://doi.org/10.1371/journal.pone.0036465
714 McGuire, K., Manuja, A., Russell, G.C., Springbett, A., Craigmile, S.C., Nichani, A.K., Malhotra,
715   D.V., Glass, E.J., 2004. Quantitative analysis of pro-inflammatory cytokine mRNA
716   expression in Theileria annulata-infected cell lines derived from resistant and susceptible
717   cattle. Vet. Immunol. Immunopathol. 99, 87–98.
718   https://doi.org/10.1016/j.vetimm.2004.01.003
719 Mikami, S., Oya, M., Kosaka, T., Mizuno, R., Miyazaki, Y., Sato, Y., Okada, Y., 2017. Increased
720   vasohibin-1 expression is associated with metastasis and poor prognosis of renal cell
721   carcinoma patients. Lab. Invest. 97, 854–862. https://doi.org/10.1038/labinvest.2017.26
722 Miyashita, H., Watanabe, T., Hayashi, H., Suzuki, Y., Nakamura, T., Ito, S., Ono, M.,
723   Hoshikawa, Y., Okada, Y., Kondo, T., Sato, Y., 2012. Angiogenesis Inhibitor Vasohibin-1
724   Enhances Stress Resistance of Endothelial Cells via Induction of SOD2 and SIRT1.
725   PLOS ONE 7, e46459. https://doi.org/10.1371/journal.pone.0046459
726 Morrison, W.I., MacHugh, N.D., Lalor, P.A., 1996. Pathogenicity of Theileria parva is influenced
727   by the host cell type infected by the parasite. Infect. Immun. 64, 557–562.
728   https://doi.org/10.1128/iai.64.2.557-562.1996
729 Mukhebi, A.W., Perry, B.D., 1992. Economic implications of the control of East Coast fever in
730   eastern, central and southern Africa, in: Proceedings of the Workshop Held in Kadoma

Hotel, Zimbabwe. International Livestock Centre for Africa (ILCA), Addis Ababa, Ethiopia.

Musoke, A.J., Nantulya, V.M., Buscher, G., Masake, R.A., Otim, B., 1982. Bovine immune response to Theileria parva: neutralizing antibodies to sporozoites. Immunology 45, 663–668.

Ndungu, S.G., Ngumi, P.N., Mbogo, S.K., Dolan, T.T., Mutugi, J.J., Young, A.S., 2005. Some preliminary observations on the susceptibility and resistance of different cattle breeds to Theileria parva infection. Onderstepoort J. Vet. Res. 72, 7–11. https://doi.org/10.4102/ojvr.v72i1.219

Neitz, W.O., 1957. Theileriosis, gonderioses and cytauxzoonoses: a review. Onderstepoort J. Vet. Res. 27.

Nemeth, M.J., Cline, A.P., Anderson, S.M., Garrett-Beal, L.J., Bodine, D.M., 2005. Hmgb3 deficiency deregulates proliferation and differentiation of common lymphoid and myeloid progenitors. Blood 105, 627–634. https://doi.org/10.1182/blood-2004-07-2551

Nemeth, M.J., Kirby, M.R., Bodine, D.M., 2006. Hmgb3 regulates the balance between hematopoietic stem cell self-renewal and differentiation. Proc. Natl. Acad. Sci. 103, 13783–13788. https://doi.org/10.1073/pnas.0604006103

Nene, V., Morrison, W.I., 2016. Approaches to vaccination against Theileria parva and Theileria annulata. Parasite Immunol. 38, 724–734. https://doi.org/10.1111/pim.12388

Nica, A.C., Dermitzakis, E.T., 2013. Expression quantitative trait loci: present and future. Philos. Trans. R. Soc. B Biol. Sci. 368, 20120362. https://doi.org/10.1098/rstb.2012.0362

Palmer, G.H., Machado, J., Fernandez, P., Heussler, V., Perinat, T., Dobbelaere, D.A.E., 1997. Parasite-mediated nuclear factor κB regulation in lymphoproliferation caused by Theileria parva infection. Proc. Natl. Acad. Sci. 94, 12527–12532. https://doi.org/10.1073/pnas.94.23.12527

Pantano, L., Hutchinson, J., Barrera, V., Piper, M., Khetani, R., Daily, K., Perumal, T.M., Kirchner, R., Steinbaugh, M., 2021. DEGreport: Report of DEG analysis. Bioconductor version: Release (3.14). https://doi.org/10.18129/B9.bioc.DEGreport

Pidugu, V.K., Pidugu, H.B., Wu, M.-M., Liu, C.-J., Lee, T.-C., 2019. Emerging Functions of Human IFIT Proteins in Cancer. Front. Mol. Biosci. 6, 148. https://doi.org/10.3389/fmolb.2019.00148

Pilotte, J., Kiosses, W., Chan, S.W., Makarenkova, H.P., Dupont-Versteegden, E., Vanderklish, P.W., 2018. Morphoregulatory functions of the RNA-binding motif protein 3 in cell spreading, polarity and migration. Sci. Rep. 8, 7367. https://doi.org/10.1038/s41598-018-25668-2

Pozzoli, U., Menozzi, G., Fumagalli, M., Cereda, M., Comi, G.P., Cagliani, R., Bresolin, N., Sironi, M., 2008. Both selective and neutral processes drive GC content evolution in the human genome. BMC Evol. Biol. 8, 99. https://doi.org/10.1186/1471-2148-8-99

Raudvere, U., Kolberg, L., Kuzmin, I., Arak, T., Adler, P., Peterson, H., Vilo, J., 2019. g:Profiler: a web server for functional enrichment analysis and conversions of gene lists (2019 update). Nucleic Acids Res. 47, W191–W198. https://doi.org/10.1093/nar/gkz369

Razmi, G., Yaghfoori, S., Mohri, M., Haghparast, A., Tajeri, S., 2019. The haematological, proinflammatory cytokines and IgG changes during an ovine experimental theileriosis. Onderstepoort J. Vet. Res. 86, 6. https://doi.org/10.4102/ojvr.v86i1.1629

Reimand, J., Kull, M., Peterson, H., Hansen, J., Vilo, J., 2007. g:Profiler—a web-based toolset for functional profiling of gene lists from large-scale experiments. Nucleic Acids Res. 35, W193–W200. https://doi.org/10.1093/nar/gkm226

Sager, H., Brunschwiler, C., Jungi, T.W., 1998. Interferon production by Theileria annulata-transformed cell lines is restricted to the beta family. Parasite Immunol. 20, 175–182. https://doi.org/10.1046/j.1365-3024.1998.00141.x

781 Saxton, R.A., Sabatini, D.M., 2017. mTOR Signalling in Growth, Metabolism, and Disease. Cell
782   168, 960–976. https://doi.org/10.1016/j.cell.2017.02.004
783 Sitt, T., Poole, E.J., Ndambuki, G., Mwaura, S., Njoroge, T., Omondi, G.P., Mutinda, M.,
784   Mathenge, J., Prettejohn, G., Morrison, W.I., Toye, P., 2015. Exposure of vaccinated and
785   naive cattle to natural challenge from buffalo-derived Theileria parva. Int. J. Parasitol.
786   Parasites Wildl. 4, 244–251. https://doi.org/10.1016/j.ijppaw.2015.04.006
787 Spooner, R.L., Innes, E.A., Glass, E.J., Brown, C.G., 1989. Theileria annulata and T. parva
788   infect and transform different bovine mononuclear cells. Immunology 66, 284–288.
789 Szklarczyk, D., Gable, A.L., Lyon, D., Junge, A., Wyder, S., Huerta-Cepas, J., Simonovic, M.,
790   Doncheva, N.T., Morris, J.H., Bork, P., Jensen, L.J., Mering, C. von, 2019. STRING v11:
791   protein–protein association networks with increased coverage, supporting functional
792   discovery in genome-wide experimental datasets. Nucleic Acids Res. 47, D607–D613.
793   https://doi.org/10.1093/nar/gky1131
794 Tindih, H.S., Geysen, D., Goddeeris, B.M., Awino, E., Dobbelaere, D.A.E., Naessens, J., 2012.
795   A Theileria parva Isolate of Low Virulence Infects a Subpopulation of Lymphocytes.
796   Infect. Immun. 80, 1267–1273. https://doi.org/10.1128/IAI.05085-11
797 Tonui, T., Corredor-Moreno, P., Kanduma, E., Njuguna, J., Njahira, M.N., Nyanjom, S.G., Silva,
798   J.C., Djikeng, A., Pelle, R., 2018. Transcriptomics reveal potential vaccine antigens and
799   a drastic increase of upregulated genes during Theileria parva development from
800   arthropod to bovine infective stages. PLOS ONE 13, e0204047.
801   https://doi.org/10.1371/journal.pone.0204047
802 Tretina, K., Gotia, H.T., Mann, D.J., Silva, J.C., 2015. Theileria-transformed bovine leukocytes
803   have cancer hallmarks. Trends Parasitol. 31, 306–314.
804   https://doi.org/10.1016/j.pt.2015.04.001
805 Tretina, K., Haidar, M., Madsen-Bouterse, S.A., Sakura, T., Mfarrej, S., Fry, L., Chaussepied,
806   M., Pain, A., Knowles, D.P., Nene, V.M., Ginsberg, D., Daubenberger, C.A., Bishop,
807   R.P., Langsley, G., Silva, J.C., 2020. Theileria parasites subvert E2F signalling to
808   stimulate leukocyte proliferation. Sci. Rep. 10, 3982. https://doi.org/10.1038/s41598-020-
809   60939-x
810 Wah, S.T., Hananantachai, H., Patarapotikul, J., Ohashi, J., Naka, I., Nuchnoi, P., 2018.
811   Interferon-induced protein with tetratricopeptide repeats 1 (IFIT1) polymorphism as a
812   genetic marker of cerebral malaria in Thai population. Asian Pac. J. Trop. Med. 11, 376.
813   https://doi.org/10.4103/1995-7645.234765
814 Wan, J., Wu, Y., Ji, X., Huang, L., Cai, W., Su, Z., Wang, S., Xu, H., 2020. IL-9 and IL-9-
815   producing cells in tumor immunity. Cell Commun. Signal. 18, 50.
816   https://doi.org/10.1186/s12964-020-00538-5
817 Wang, H., Deng, Q., Lv, Z., Ling, Y., Hou, X., Chen, Z., Dinglin, X., Ma, S., Li, D., Wu, Y., Peng,
818   Y., Huang, H., Chen, L., 2019. N6-methyladenosine induced miR-143-3p promotes the
819   brain metastasis of lung cancer via regulation of VASH1. Mol. Cancer 18, 181.
820   https://doi.org/10.1186/s12943-019-1108-x
821 Watanabe, K., Taskesen, E., van Bochoven, A., Posthuma, D., 2017. Functional mapping and
822   annotation of genetic associations with FUMA. Nat. Commun. 8, 1826.
823   https://doi.org/10.1038/s41467-017-01261-5
824 Webster, G.A., Perkins, N.D., 1999. Transcriptional Cross Talk between NF-κB and p53. Mol.
825   Cell. Biol. 19, 3485–3495. https://doi.org/10.1128/MCB.19.5.3485
826 Wellmann, S., Truss, M., Bruder, E., Tornillo, L., Zelmer, A., Seeger, K., Bührer, C., 2010. The
827   RNA-Binding Protein RBM3 Is Required for Cell Proliferation and Protects Against
828   Serum Deprivation-Induced Cell Death. Pediatr. Res. 67, 35–41.
829   https://doi.org/10.1203/PDR.0b013e3181c13326
830 Wragg, D., Cook, E.A.J., Laté, P.L. de, Sitt, T., Hemmink, J.D., Chepkwony, M.C., Njeru, R.,

831   Poole, E.J., Powell, J., Paxton, E.A., Callaby, R., Talenti, A., Miyunga, A.A., Ndambuki,
832   G., Mwaura, S., Auty, H., Matika, O., Hassan, M., Marshall, K., Connelley, T., Morrison,
833   L.J., Bronsvoort, B.M. deC, Morrison, W.I., Toye, P.G., Prendergast, J.G.D., 2022. A
834   locus conferring tolerance to Theileria infection in African cattle. PLOS Genet. 18,
835   e1010099. https://doi.org/10.1371/journal.pgen.1010099
836 Yamada, S., Konnai, S., Imamura, S., Simuunza, M., Chembensofu, M., Chota, A., Nambota,
837   A., Onuma, M., Ohashi, K., 2009. Quantitative analysis of cytokine mRNA expression
838   and protozoan DNA load in Theileria parva-infected cattle. J. Vet. Med. Sci. 71, 49–54.
839   https://doi.org/10.1292/jvms.71.49
840 Yang, W., Tanaka, Y., Bundo, M., Hirokawa, N., 2014. Antioxidant Signalling Involving the
841   Microtubule Motor KIF12 Is an Intracellular Target of Nutrition Excess in Beta Cells. Dev.
842   Cell 31, 202–214. https://doi.org/10.1016/j.devcel.2014.08.028
843 Zhao, G., Na, R., Li, L., Xiao, H., Ding, N., Sun, Y., Han, R., 2017. Vasohibin-1 inhibits
844   angiogenesis and suppresses tumor growth in renal cell carcinoma. Oncol. Rep. 38,
845   1021–1028. https://doi.org/10.3892/or.2017.5746
846 Zou, J., Li, Z., Deng, H., Hao, J., Ding, R., Zhao, M., 2019. TMEM213 as a novel prognostic and
847   predictive biomarker for patients with lung adenocarcinoma after curative resection: a
848   study based on bioinformatics analysis. J. Thorac. Dis. 11.
849   https://doi.org/10.21037/jtd.2019.08.01

850

851

852 **Figure legends**

853

854 Fig 1: Global change in transcript sequence content divergence following infection. (A) Median

855 nucleotide base sequence content across samples at day 0, 7 and 15. (B) Comparison of GC

856 content across base positions 20 to 40 between day 0, 7 and 15. The difference in GC content

857 was significant (Wilcoxon $p < 0.05$) in all comparisons. (C) Genes whose expression level

858 exceeds the 50th percentile for each day, plotted as log normalised expression against %GC

859 content with regression lines showing increase in GC content of these most highly expressed

860 genes post-infection. Marginal box plots indicate a significant shift in GC content (Wilxcoxon $p <$

861 0.05) post-infection. (D) Genes were grouped into three equal content sized bins based on day

862 0 expression levels (low, medium, high), and the ratio of normalised expression levels between

863 days 15 and 0 logged and plotted against GC content, confirming the relationship between GC

864 content and expression level change, particularly among the genes more highly expressed pre-

865   infection. Horizontal dashed lines in panel D indicate the 5th and 95th percentiles of the

866   normalised expression data.

867

868   Fig 2: Proportion of reads mapping to the *T. parva* genome relative to all reads mapped. (A) The

869    $\log_{10}$ number of reads mapped to the *T. parva* genome versus all reads mapped. Differences in

870   the total number of reads mapped between time points were not significant, whereas there was

871   a significant difference in the number of reads mapping to *T. parva* between each time point,

872   with the most significant increase from day 0 to day 15 (Wilcoxon p = 1 x 10^{-15}). (B) The

873   proportion of reads mapped to the *T. parva* genome grouped by survival outcome. Comparison

874   of means between animals that succumbed or were treated to those that survived infection

875   returns a Wilcoxon p of 0.076.

876

877   Fig 3: PCA of normalised gene expression data. Each circle represents a sample from an

878   individual animal at a specific time point, as indicated.

879

880   Fig 4: Trends of host gene expression in response to field exposure to *T. parva*. (A) Heatmap of

881   significantly differentially expressed genes across sampling time points. The heatmap is scaled

882   by column with each row representing an individual sample and each column representing a

883   gene. The genes cluster into 4 groups, as denoted above the heatmap. (B) Antagonistic

884   expression patterns of *NFkB* and *P53* proteins across the time course. (C) The expression

885   patterns of *IL2* and its receptors (*IL2RA*, *IL2RB*, *IL2RG*) across time.

886

887   Fig 5: (A-F) Expression profiles of the six genes significantly differentially expressed between

888   the survivors and deceased animals at day 15 as well as across the entire time course. (G)

889   Expression profile of IL9.

890

891   Fig 6: Functional enrichment analysis of genes differentially expressed at the three time points

892   in cattle that survived versus those that succumbed to infection with *T. parva.* The gene sets

893   used for the analysis in this were termed as upregulated or down regulated in the tolerant group

894   based on the fold change observed. The gene sets were identified via functional enrichment

895   analyses using FUMA and DAVID. The input genes were those with a nominal p value < 0.01

896   following differential gene expression analyses. The results of the enrichment analyses were

897   retained if they had an FDR < 0.05.

898

899   Fig 7: Example of a significant response expression quantitative trait loci (reQTL) for *RTN4IP1*.

900   The expression of *RTN4IP1* is significantly correlated with allele dosage at SNP 9:43255137.

901   Beta comparisons indicate a significant change in the regression slope following infection,

902   revealing the eQTL to be a response eQTL. The expression of *RTN4IP1* is nominally

903   significantly (ANOVA p < 0.05) higher at day 15 in animals that survived infection compared to

904   those that succumbed. RTN4IP1 was not among the significant DEGs following (FDR)

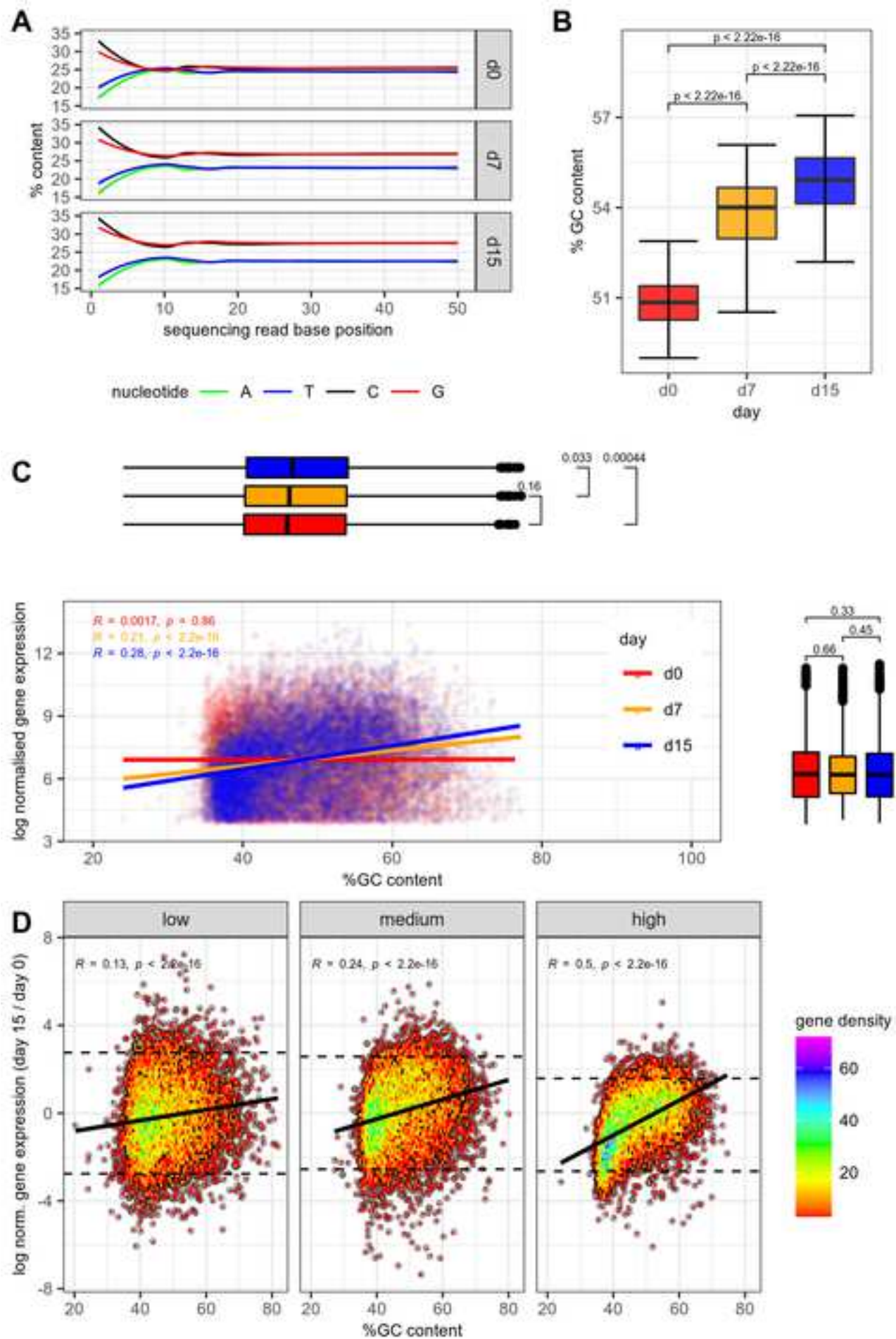905   correction for multiple testing.
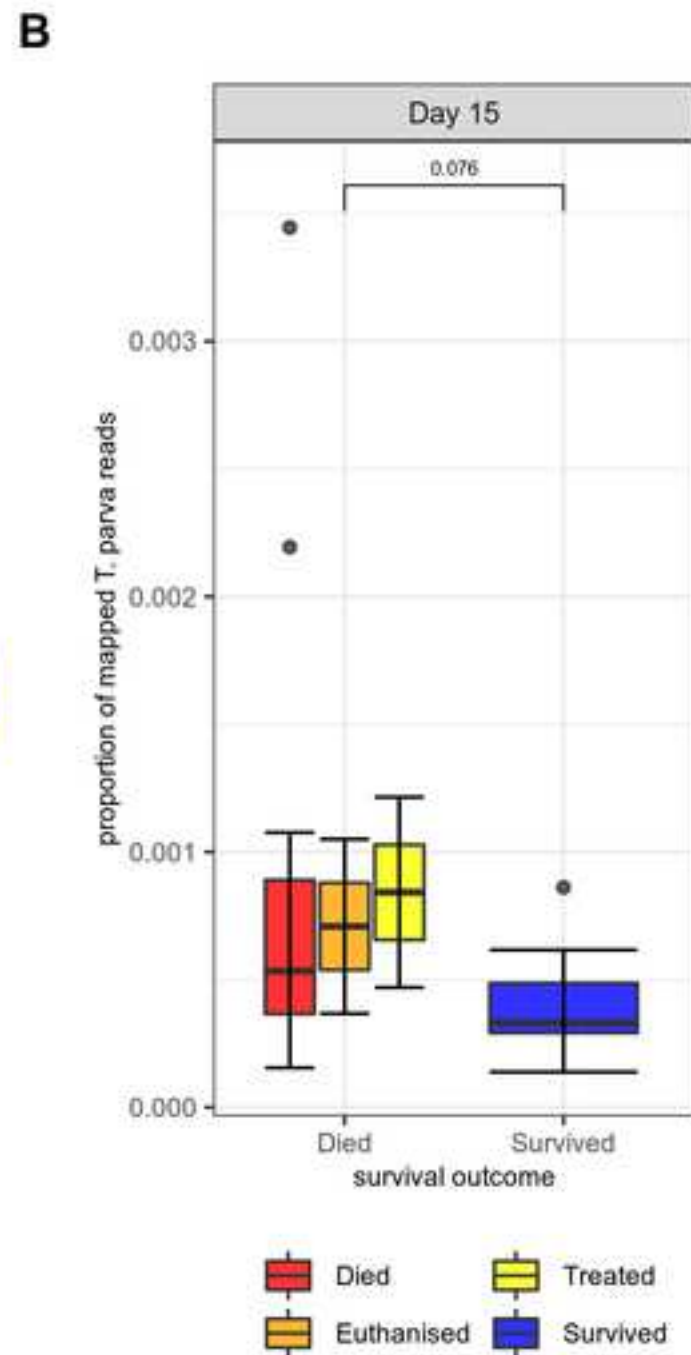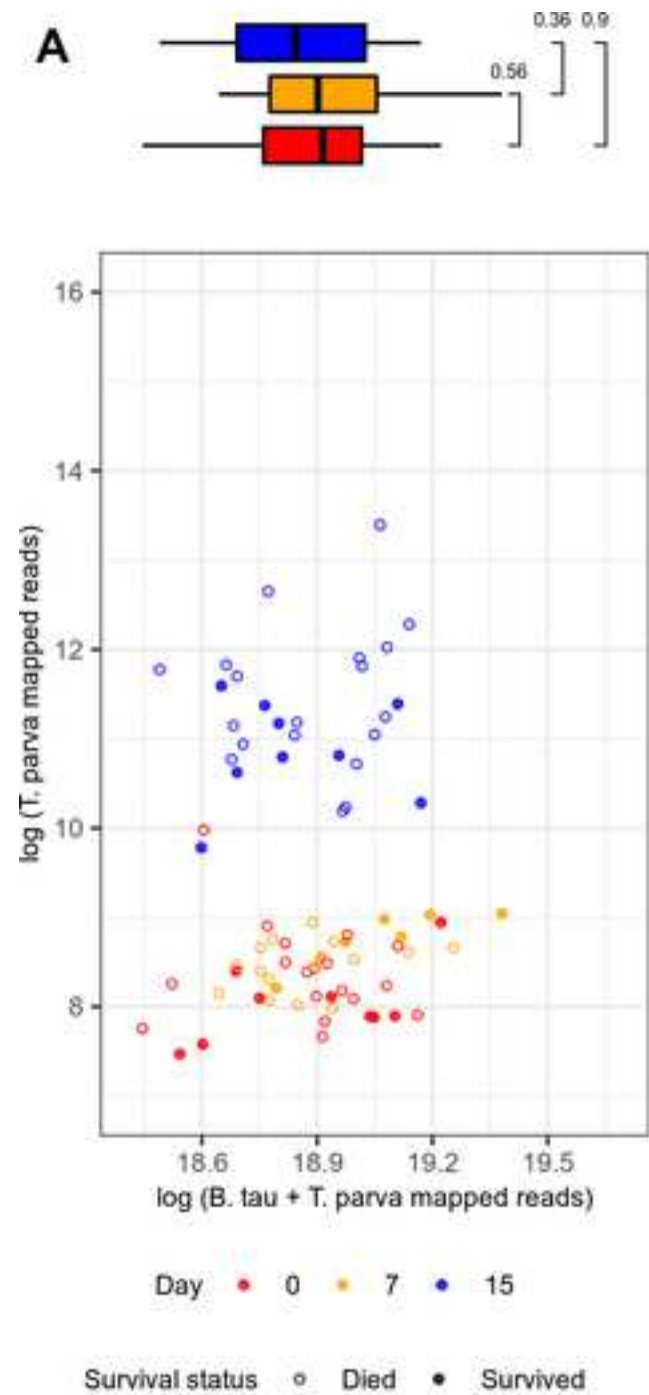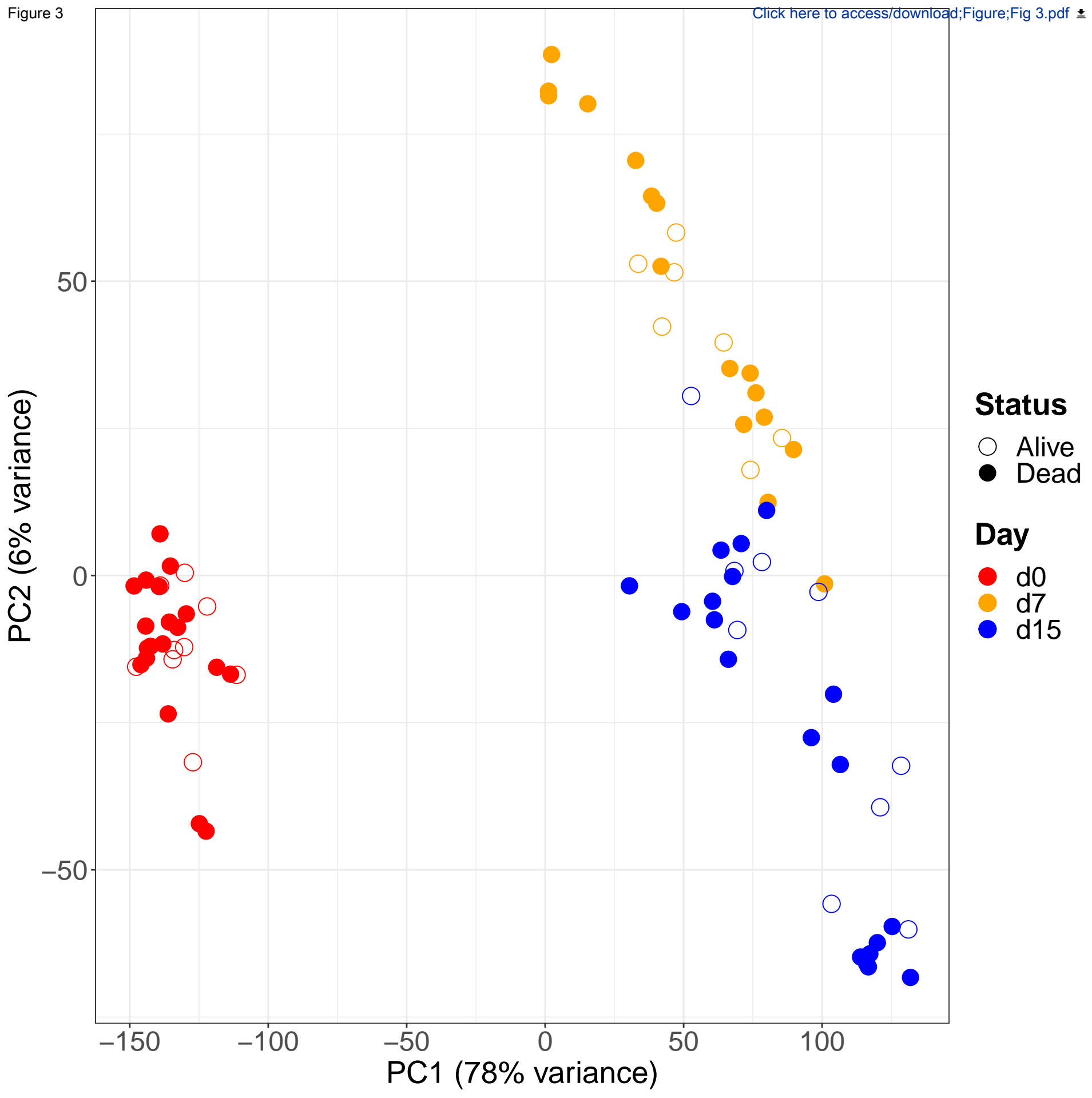
906

907

908

909

Figure 1   Click here to access/download;Figure;Fig 1.png ±

Figure 2   Click here to access/download;Figure;Fig 2.png ⬇

Figure 3

Figure 4

Figure 5

Click here to access/download;Figure;Fig 5.pdf ⬇

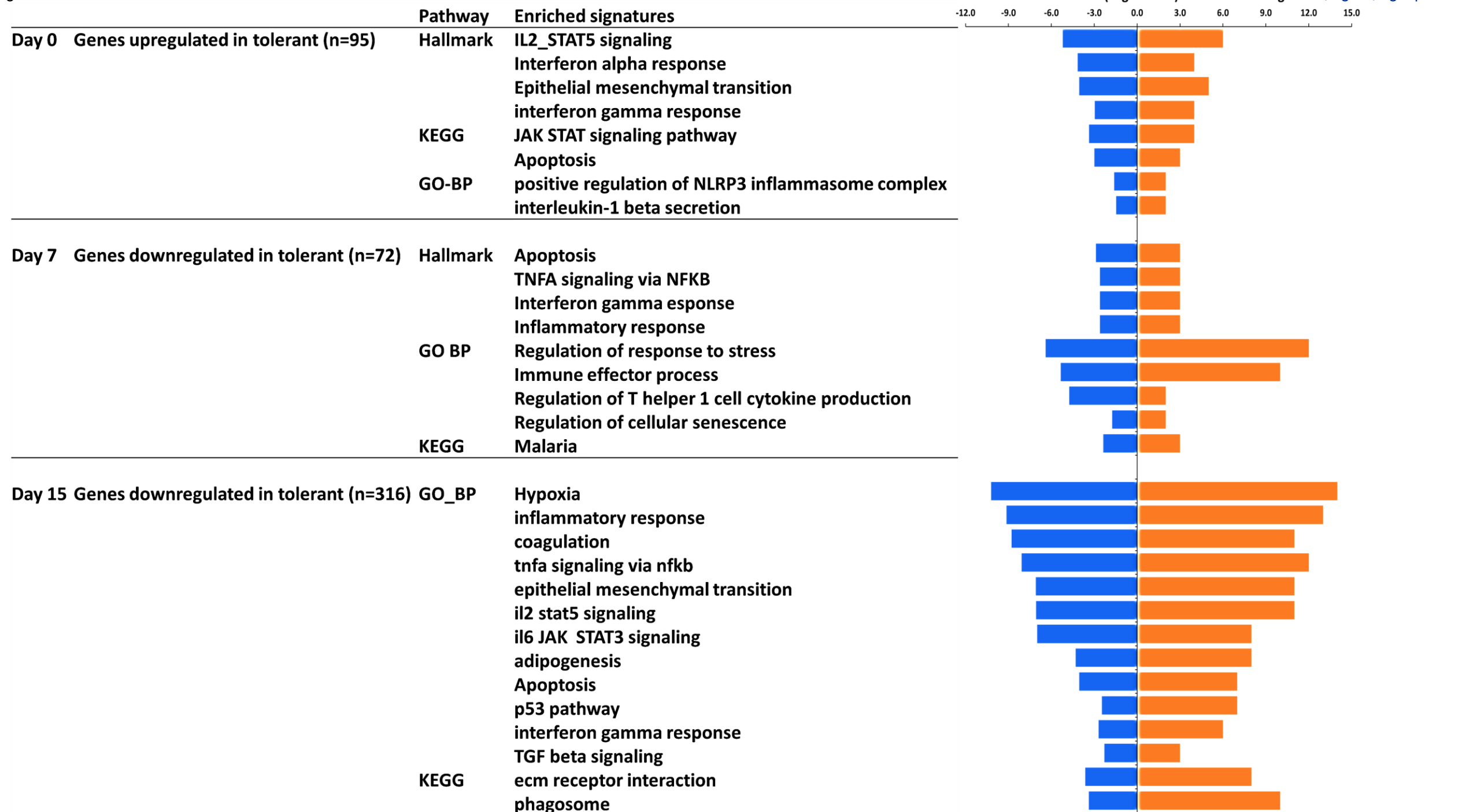Figure 5

Figure 6

Figure 7

Click here to access/download;Figure;Fig 7.png ±
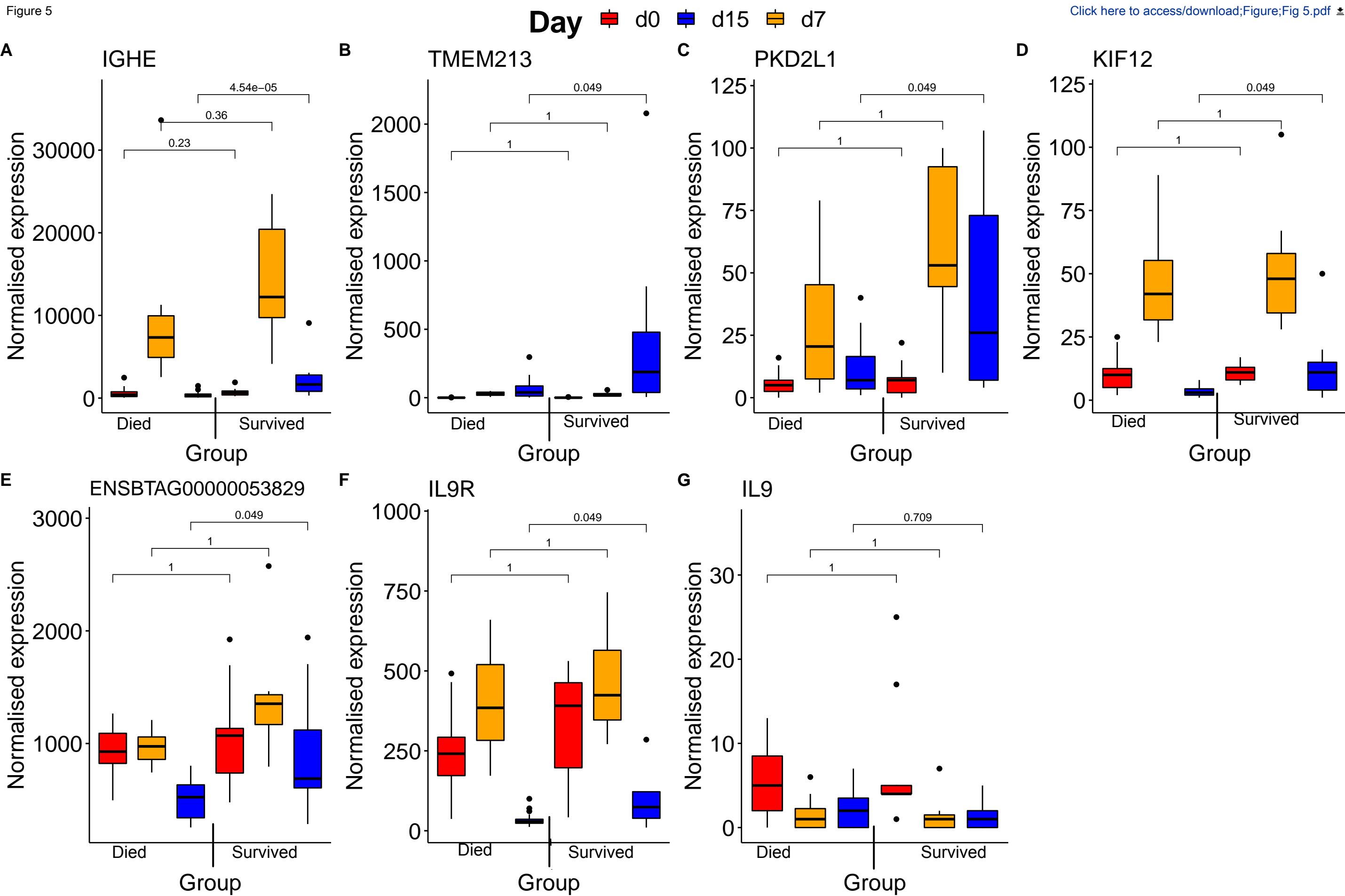
SNP: 9:43255137; Gene: RTN4IP1
reQTL beta comparisons: 0:7 Z = -5.95; 7:15 Z = 1.76; 0:15 Z = -5.75